


 Cite this: *RSC Adv.*, 2026, **16**, 4004

Resource utilization of urban sludge *via* pyrolysis: impacts on cement performance and environmental safety

Fangzhen Hu, * Shanjun Zhang and Jing Liu

This work utilizes pyrolysis technology to convert urban sludge into a pyrolyzed sludge at temperatures ranging from 300 °C to 600 °C and investigates its potential application in cement-based materials. The results showed that as the pyrolysis temperature increases, the yield of the pyrolyzed sludge decreases (from 73.7% to 58.7%), while the ash content and specific surface area increase (specific surface area increases from 11.9 m² g⁻¹ to 186.5 m² g⁻¹). The pH shifts from neutral to alkaline (approximately 6.9 to 9.5), indicating that the product is more stable and possesses a good porous structure. Performance tests reveal that untreated sludge significantly delays cement setting and reduces compressive strength (with a 10% dosage, the 3 days strength is only 11.5 MPa), whereas pyrolyzed sludge significantly improves mechanical properties. At an appropriate dosage, the 3 days strength increases by approximately 37%, and the 28 days strength improves by up to 35%. Pyrolyzed urban sludge (600 °C, 3–5%) significantly improved splitting tensile strength, while untreated sludge and higher replacement ratios reduced it. Environmental risk assessment shows that although the pyrolysis process concentrates heavy metals, the leaching concentrations of all metals in the concrete are well below the limits specified in GB 5085.3-2007, indicating that the environmental risks are controllable. In conclusion, pyrolysis not only enables the reduction and stabilization of sludge but also enhances its performance in concrete, demonstrating that pyrolyzed sludge is a feasible resource utilization approach as cement admixtures.

Received 4th October 2025

Accepted 12th January 2026

DOI: 10.1039/d5ra07550e

rsc.li/rsc-advances

1 Introduction

The quantity of sludge generated by urban sewage treatment plants has increased rapidly with urbanization and the construction of wastewater treatment facilities.¹ Municipal sludge typically contains high moisture, large amounts of organic matter, and various inorganic components, as well as pathogens and heavy metals.² If sludge is not properly treated, conventional disposal options such as landfilling, land application and simple incineration may cause secondary pollution.^{3,4} Landfilling occupies valuable land resources and may lead to the leaching of organic contaminants and heavy metals into soil and groundwater.⁵ Land application can recycle nutrients, but its long-term use is restricted by sanitary concerns and the risk of heavy-metal accumulation.^{6,7} Incineration can significantly reduce the volume of sludge and recover part of its energy content, but the process is energy-intensive and the generated ash still requires safe disposal. Consequently, achieving simultaneous stabilization, harmless treatment and resource utilization of urban sludge has become a critical issue in environmental engineering.

Among the various emerging sludge treatment technologies, pyrolysis has attracted increasing attention due to its high volume-reduction efficiency and its potential to convert sludge into value-added products.^{4,8} During pyrolysis, organic matter in the sludge is thermally decomposed under oxygen-limited conditions, yielding a solid residue rich in mineral components (sludge-derived biochar), together with gaseous and liquid products.^{9,10} The solid pyrolyzed sludge can be used in the construction industry as a cementitious or filler material, enabling long-term immobilization of the inert components and heavy metals within a cement matrix.⁷ Previous studies have shown that sludge-derived char may partially replace cement or aggregates in concrete, mortar or bricks, and that the alkaline environment of cement-based materials can further stabilize heavy metals and reduce their leaching risk.¹¹ In addition, the inorganic phases in the pyrolyzed sludge (e.g., silica and alumina) may exhibit pozzolanic activity or micro-filling effects, potentially improving certain mechanical properties of cementitious materials.⁹ However, most existing research is limited in two important aspects. First, many studies adopt a single pyrolysis temperature or a narrow temperature range, making it difficult to elucidate the systematic influence of pyrolysis temperature on the physicochemical properties of pyrolyzed sludge and their subsequent performance in cement systems.^{10,12} Second, previous work often focuses primarily on

School of Architectural Engineering, Wuhan City Polytechnic, Wuhan 430068, China.
 E-mail: 02009028@whcp.edu.cn



mechanical properties (such as setting time or strength), while the environmental safety aspects—especially the evolution of total and leachable heavy metals in cementitious matrices—are less comprehensively addressed.¹³ As a result, there is still a lack of integrated evaluations that couple the thermal evolution of sludge, the multiscale performance of cement-based materials, and the environmental risk of heavy metals under different pyrolysis conditions.

Based on these considerations, this study investigates the potential of municipal sludge pyrolyzed at 300~600 °C for application in cement-based materials. The physicochemical evolution of the sludge biochar (e.g., yield, pore structure, and composition) was first characterized. Subsequently, cement pastes with varying char dosages were evaluated for setting time, compressive strength, and splitting tensile strength. Finally, the environmental safety was assessed by determining the total content and leaching toxicity of heavy metals (Cu, Cr, Ni, Cd, Pb, Zn, and As). This integrated approach is novel in that it (i) provides a multi-temperature comparison of sludge pyrolysis products in cement systems and (ii) couples mechanical performance with heavy metal immobilization to identify optimal pyrolysis conditions and replacement levels that simultaneously satisfy mechanical and environmental requirements.

2 Materials and methods

2.1 Materials and reagents

The primary raw material for this experiment was P·O 42.5 Portland cement. The sludge was sourced from the Wuhan wastewater treatment plant (Hubei Province, China). Prior to the experiment, the raw sludge was dried in a laboratory constant temperature oven at 105 °C for 24 h, then ground separately using a multifunctional grinder. The prepared raw materials were stored in sealed bags for later use.

2.2 Preparation of pyrolyzed sludge

The sludge (SS), which had been air-dried outdoors, was placed in an oven and dried to a constant weight. Afterward, it was crushed into powder using a grinder and then transferred into clean crucibles with lids, maintaining a low-oxygen environment. The crucibles were then placed in a programmable muffle furnace (KSMF-2000). The temperature was set to increase at a rate of 20 °C min⁻¹, following the pyrolysis procedures outlined in previous studies on pyrolyzed sludge, and the SS was pyrolyzed at temperatures ranging from 300 to 600 °C. After maintaining the specified temperature for 2 h, the pyrolyzed sludge was removed and allowed to cool naturally to room temperature in a ventilated area. The pyrolyzed sludge was then ground into powder using a ball mill and stored in dry, light-blocking bottles in a cool and dry place. The dried SS was pyrolyzed at 300, 500 and 600 °C, and the resulting products were denoted as SS300, SS500 and SS600, respectively. Subsequently, SS300, SS500 and SS600 were incorporated into cement paste as partial cement replacements to compare the effects of sludge pyrolysis at different temperatures on hydration

behavior, mechanical properties and heavy metal immobilization.

2.3 Experimental methods

2.3.1 Setting time. To assess the effect of different sludges and their pyrolyzed sludge on the cement hydration process, the setting time method was used to test the initial and final setting times of cement. P·O 42.5 Portland cement was used as the baseline, and control paste without sludge or pyrolyzed sludge (CK), untreated SS and pyrolyzed sludge (SS300, SS400, SS500, SS600) were used as partial substitutes for the cement. The dosage range was set at 1%, 3%, 5%, and 10%. The cement was thoroughly mixed with sludge or pyrolyzed sludge in the specified proportions, and deionized water was added to obtain a standard-consistency cement paste. The standard consistency water requirement and the corresponding water-to-binder ratio (w/b = 0.40) were determined in advance according to GB/T 1346-2011.¹⁴ The initial and final setting times of the standard-consistency paste were then measured using a Vicat apparatus, in accordance with GB/T 1346-2011, and the effects of different admixtures on cement setting behavior were compared.

2.3.2 Preparation of cement specimens. To evaluate the effect of different admixtures on the cement strength, cement paste specimens were prepared using different types of sludge and pyrolysis products as substitutes for cement. Standard P·O 42.5 Portland cement and pyrolyzed sludge obtained at different temperatures (300 °C, 400 °C, 500 °C and 600 °C) were used as admixtures. The SS or pyrolyzed sludge were mixed with cement in varying proportions (1%, 3%, 5% and 10% by mass of binder), and deionized water was then added at a constant water-to-binder ratio (w/b = 0.40) for all mixtures. The paste was stirred until homogeneous and cast into standard molds, vibrated to remove entrapped air, and cured in a humid environment at room temperature for 3 days and 28 days before the compressive strength tests. The compressive strength of the specimens was measured at 3 days and 28 days using a compressive testing machine.

2.3.3 Leaching test. To evaluate the environmental risk of heavy metals in cement-based materials, the TCLP method was used to determine the leaching concentration of heavy metals in concrete with different admixtures. Following the standard TCLP leaching method, an acetic acid buffer solution with a pH of 4.93 ± 0.05 was prepared. The volume ratio of leachate to cement specimen mass was 20 : 1 (mL g⁻¹). The cement specimens were removed after 28 days of curing, and then cut to ensure a smooth surface and consistent mass. The cut specimens were placed in containers, and acetic acid buffer solution was added. The containers were sealed, and the specimens were shaken at a constant temperature of 25 °C for 24 h. After leaching, solid particles were removed using filtration to obtain the leachate.

The leachate was analyzed for Cu, Cr, Ni, Cd, Pb, Zn, and As content using an inductively coupled plasma mass spectrometer (ICP-MS, Shimadzu ICPE-9000, Japan). The heavy metal leaching concentrations were compared with the limit values



Table 1 Limit values of hazardous components in leachate (mg L⁻¹)

Cu	Cr	Ni	Cd	Pb	Zn	As
<100	<15	<5	<1	<5	<100	<5

(Table 1) in the Identification Standard for Hazardous Waste: Leachability Toxicity Identification (GB/T 5085.3-2007) to assess whether the concrete containing sludge and pyrolyzed sludge qualifies as a leachability toxic hazardous waste.¹⁵

After 28 days of curing, the hardened cement specimens were crushed and ground to pass a 0.075 mm sieve. Approximately 0.20 g of the powdered sample was accurately weighed into a digestion vessel, and a mixed acid solution of HNO₃-HCl (3 : 1, v/v) was added. The mixture was heated on a hot plate until the residue became clear and nearly colorless, then cooled, diluted with deionized water and filtered into a volumetric flask. The resulting solutions were analyzed for Cu, Cr, Ni, Cd, Pb, Zn and As by ICP-OES.

3 Results and discussion

3.1 Physicochemical properties analysis

Table 2 provides an overview of the properties of sludge and pyrolyzed sludge was provided. As the pyrolysis temperature increased from 300 °C to 600 °C, the yield of pyrolyzed sludge decreased markedly from 73.69% to 58.71%. At the same time, the ash content increased from 46.74% to 83.79%, and the volatile matter content decreased from 48.28% to 6.84%. This trend was consistent with literature reports: higher pyrolysis temperatures promoted the removal of moisture and volatiles, which decreased the yield of the pyrolyzed sludge and increased the residual ash content.¹ At elevated temperatures, the organic matter in the sludge underwent pyrolysis, leading to the release of a substantial amount of volatile components (resulting in a decrease in volatile matter).⁶ Meanwhile, the proportion of inorganic minerals in the residue increased (causing a rise in

ash content), which contributed to a notable reduction in the yield of the pyrolyzed sludge.⁴ As the pyrolysis temperature increased, the pH of the pyrolyzed sludge rose from 6.87 in SS to 9.47 in SS600, indicating a distinct transition from neutral-acidic to alkaline. The literature suggests that pyrolyzed sludge produced through high-temperature pyrolysis exhibited enhanced alkalinity, as the removal of acidic functional groups and the enrichment of mineral components led to an increase in alkaline functional groups in the pyrolyzed sludge.^{5,9,16}

In terms of elemental composition, pyrolysis resulted in a continuous decrease in the contents of C, H, N, and O. For instance, C decreased from 19.65% to 10.48%, and H dropped from 3.02% to 0.53%. This suggested that at high temperatures, the volatile elements in the sludge were largely decomposed and lost. The literature also reported that as the temperature increased, the contents of C, H, N, and O in the pyrolyzed sludge structure significantly decreased.^{6,7,16} Although the proportion of residual C in the pyrolyzed sludge decreased, it tended to form more aromatic structures (as evidenced by the atomic ratio analysis below), and the reduction in N content also indicated that nitrogen escaped in the form of volatile matter or gas. The H/C ratio decreased from 0.15 in SS to 0.05 in SS600, and the O/C ratio dropped from 0.78 to 0.31. The decrease in both the H/C and O/C ratios reflects a relative reduction in hydrogen and oxygen content, along with an increase in the aromaticity of the carbon structure. The literature indicated that high-temperature pyrolysis significantly reduced the H/C ratio of pyrolyzed sludge, suggesting that the carbon skeleton became more saturated and stable, with enhanced aromatic clusters.^{3,12} Pyrolyzed sludge with low H/C and low O/C ratios generally exhibited higher carbon fixation stability, making it more resistant to microbial and oxidative decomposition, thus facilitating long-term carbon storage.

As the pyrolysis temperature increased, the surface area of the pyrolyzed sludge rose sharply, from 11.88 m² g⁻¹ in the original sludge to 186.53 m² g⁻¹ in SS600. The literature reports that high-temperature pyrolysis significantly expanded the surface area and porosity of pyrolyzed sludge. The micropore

Table 2 Analysis of the physical properties of sludge and sludge-derived products

	SS	SS300	SS400	SS500	SS600
Yield (%)	—	73.69 ± 3.18	67.82 ± 2.04	62.16 ± 1.74	58.71 ± 1.64
Ash (%)	46.74 ± 0.58	53.69 ± 1.19	67.37 ± 1.42	78.09 ± 1.44	83.79 ± 1.57
Volatile matter (%)	48.28 ± 1.19	25.47 ± 0.96	17.92 ± 2.07	11.59 ± 1.06	6.84 ± 0.74
pH	6.87 ± 0.13	7.67 ± 0.27	8.32 ± 0.31	8.96 ± 0.21	9.47 ± 0.12
C (%)	19.65	16.62	13.62	11.63	10.48
H (%)	3.02	2.11	1.07	0.86	0.53
N (%)	2.27	1.85	1.04	0.76	0.34
O (%)	15.32	10.70	7.84	5.22	3.28
H/C (%)	0.15	0.13	0.08	0.07	0.05
O/C (%)	0.78	0.64	0.58	0.45	0.31
Surface area (m ² g ⁻¹)	11.88	59.82	104.82	156.28	186.53
Micropore surface area (m ² g ⁻¹)	4.21	6.53	7.15	6.58	6.43
External surface area (m ² g ⁻¹)	7.67	53.29	97.67	149.70	180.10
Total pore volume (cm ³ g ⁻¹)	0.12	0.36	0.40	0.65	0.71
Micropore volume (cm ³ g ⁻¹)	0.23 × 10 ⁻²	0.27 × 10 ⁻²	0.28 × 10 ⁻²	0.15 × 10 ⁻²	0.15 × 10 ⁻²
Average pore diameter (nm)	41.24	23.89	15.22	13.52	10.53



surface area showed little change, peaking slightly at $7.15 \text{ m}^2 \text{ g}^{-1}$ at 400°C , while the external surface area continued to increase with temperature, reaching $180.10 \text{ m}^2 \text{ g}^{-1}$ at SS600. The total pore volume also increased, from $0.36 \text{ cm}^3 \text{ g}^{-1}$ at SS300 to $0.71 \text{ cm}^3 \text{ g}^{-1}$ at SS600, with the micropore volume decreasing slightly after reaching a maximum value at the medium-temperature stage (400°C). This suggested that some micropores may have merged to form larger pore sizes at higher temperatures.² The average pore diameter decreased from 41.2 nm in SS to 10.5 nm in SS600, demonstrating that pyrolysis shifted the pore size distribution toward smaller scales. This indicated that increasing the pyrolysis temperature favored the formation of larger pore volumes and surface areas in pyrolyzed sludge. The reasons for this were as follows: first, the higher the pyrolysis temperature, the more volatile substances were produced, which led to the formation of larger pore volumes and surface areas;^{5,6} second, high temperatures caused the collapse of the original pore structure, forming larger pores.^{9,16} Therefore, higher pyrolysis temperatures resulted in larger surface areas and pore volumes. Overall, high-temperature pyrolysis produced pyrolyzed sludge with abundant micropores and large surface areas.

3.2 Structural characterization of pyrolyzed sludge

To further determine the effect of pyrolysis temperature on the surface morphology and pore structure of pyrolyzed sludge, a comparative analysis of the morphology of the original sludge and pyrolyzed sludge was performed (Fig. 1). The original dried sludge exhibited a plate-like layered structure under SEM, with a smooth and dense surface (Fig. 1a). When the pyrolysis temperature was 300°C (Fig. 1b), cracks began to appear on the pyrolyzed sludge surface, and tar-like aggregates were visible adhering to the particle surface, making the local morphology slightly rough. As the temperature continued to rise to 400°C

(Fig. 1c and d), the original dense structure gradually fragmented and dispersed, forming particulate debris with obvious pores and cavities, resulting in a looser, more porous structure. At 600°C pyrolysis (Fig. 1e), most of the volatile organic matter was completely removed, and the product exhibited a highly porous and rough surface structure with numerous cracks and deep pores penetrating the particle surface. Overall, with increasing pyrolysis temperature, the sludge particles transitioned from the original dense and smooth state to a fragmented, dispersed, and porous rough form, with a significant increase in the number of cracks and pores, while surface aggregation phenomena weakened.

The FTIR spectrum of pyrolyzed sludge is shown in Fig. 2a. The absorption peak in the range of $3240\text{--}3460 \text{ cm}^{-1}$ was attributed to the stretching vibration of $-\text{OH}$ groups.¹⁷ As the pyrolysis temperature increased from 300°C to 600°C , the intensity of this peak gradually weakened, indicating that hydroxyl-related functional groups decomposed at high temperatures. The stretching vibration peaks of aliphatic $-\text{CH}_3$ appeared at 2930 and 2853 cm^{-1} , but they were almost absent in the 300°C pyrolysis sample (SS300), suggesting that unstable aliphatic alkyl structures easily decomposed during pyrolysis, releasing small molecule gases such as methane and carbon dioxide.³ This reflected that the pyrolysis process was primarily a dehydrogenation-condensation process, resulting in the formation of stable aromatic structures.⁸ The $\text{C}=\text{O}$ vibration peak at 1655 cm^{-1} in the original sludge shifted to 1630 cm^{-1} after pyrolysis and gradually weakened with increasing temperature.¹³ In the pyrolyzed sludge, the characteristic peak at 1540 cm^{-1} corresponded to the stretching vibration of $-\text{COOH}$, while the $-\text{CH}_2$ -related absorption peaks at 1460 cm^{-1} and 1403 cm^{-1} almost disappeared. The peak observed near 1032 cm^{-1} was attributed to $\text{C}-\text{O}$ stretching vibrations or $\text{Si}-\text{O}$ bonds, and this feature remained present at 600°C , indicating the formation of quartz structures and stable $\text{C}-\text{O}$ bonds in

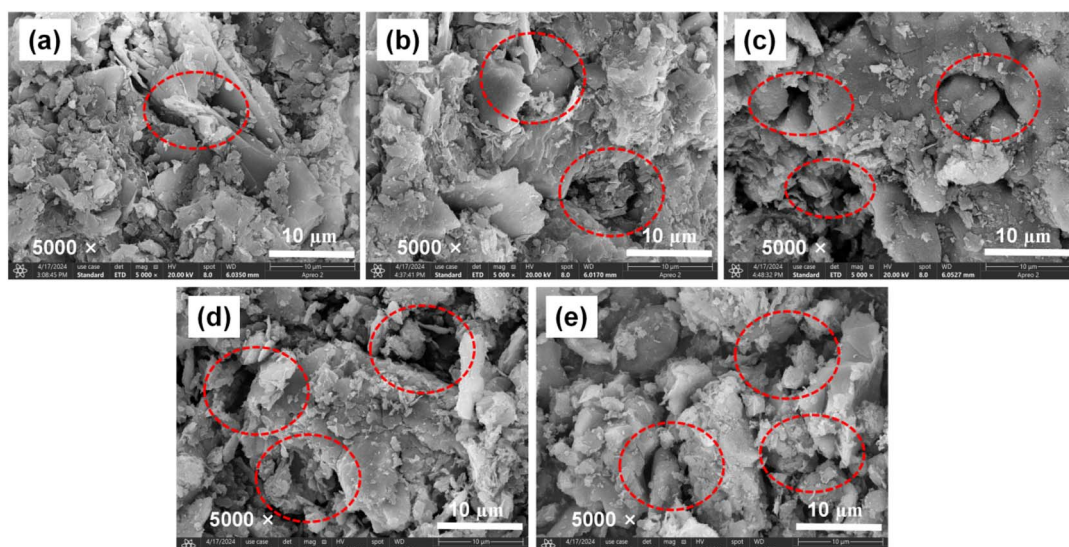


Fig. 1 Morphological images of dried municipal sludge and sludge-derived products obtained at different pyrolysis temperatures (a: SS, b: SS300, c: SS400, d: SS500 and e: SS600). The red dashed circle in SEM represents pore or gully structures.



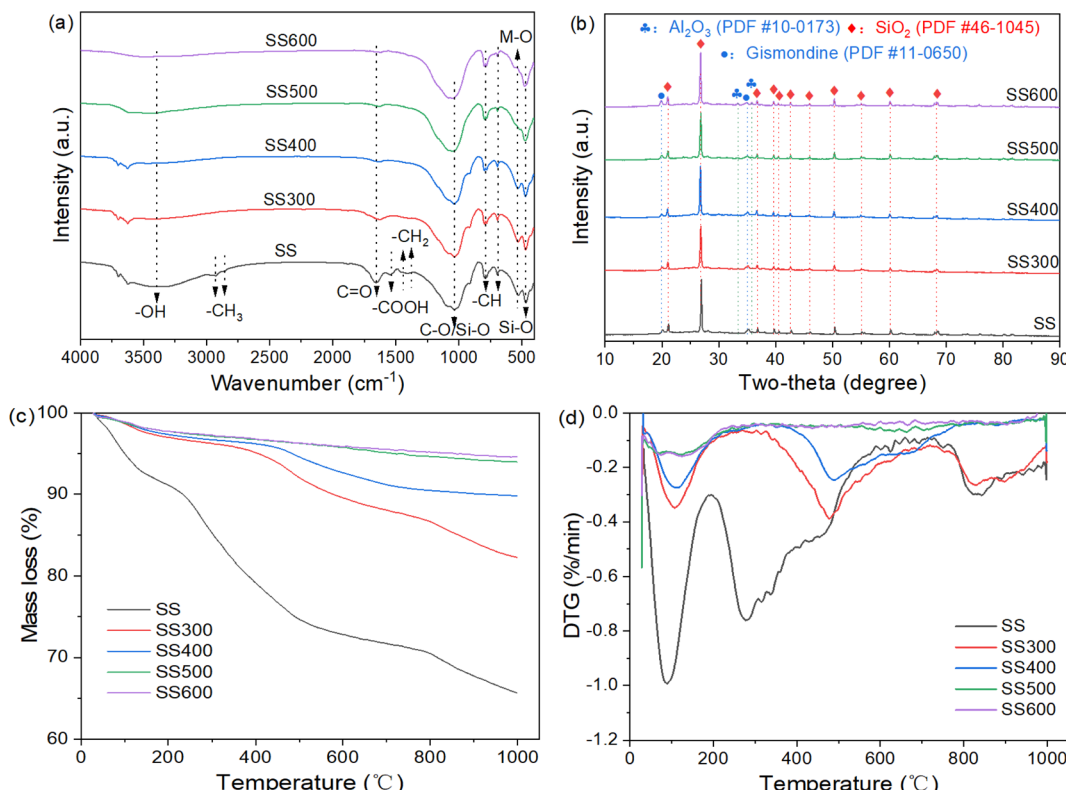


Fig. 2 FTIR (a), XRD (b), TG (c), and DTG (d) analyses of dried sludge and pyrolyzed sludge.

pyrolyzed sludge.¹¹ The absorption peaks in the 800–600 cm^{-1} range corresponded to aromatic or heterocyclic aromatic compounds ($-\text{CH}_2$), and they were still clearly visible at 600 $^{\circ}\text{C}$, suggesting that such aromatic structures were relatively stable.¹⁶ Additionally, the absorption peak at 633 cm^{-1} was attributed to the stretching vibration of R-M (where M was a metal element) in metal compounds, which weakened with increasing temperature, indicating that some metal compounds decomposed at high temperatures. The characteristic peak at 470 cm^{-1} corresponded to Si-O vibrations.^{4,9}

X-ray diffraction (XRD) analysis was carried out to identify the crystalline mineral phases in the dried sludge and pyrolyzed sludge (Fig. 2b). The results showed that the main crystalline phases in the original sludge and pyrolyzed sludge were SiO_2 (PDF#46-1045) and Gismondine ($\text{CaAl}_2\text{Si}_2\text{O}_4 \cdot 4\text{H}_2\text{O}$, PDF#11-0650).¹⁷ As the pyrolysis temperature increased to 500 $^{\circ}\text{C}$ and 600 $^{\circ}\text{C}$, characteristic peaks of alumina (Al_2O_3 , PDF#10-0173) gradually appeared and the intensity of gismondine peaks decreased, indicating that gismondine partially decomposed and transformed into Al-containing oxide phases under high-temperature conditions.⁹ However, the overall changes in peak intensity remained relatively subtle, which can be attributed to the predominance of amorphous phases and the low proportion of crystalline minerals in the sludge, as well as dilution of crystalline phases by the glassy matrix after pyrolysis.

The TG (Fig. 2c) and DTG (Fig. 2d) curve of the original sludge could be divided into four stages. Stage I (room temperature–200 $^{\circ}\text{C}$) primarily involved the volatilization of free

and bound water, with a mass loss of about 8.9%.⁵ Stage II (200–400 $^{\circ}\text{C}$) corresponded to the decomposition and volatilization of organic matter (proteins, fats, and easily degradable organic substances), with a loss of about 12.0%.⁵ Stage III (400–600 $^{\circ}\text{C}$) involved the slow cracking of some hemicellulose/cellulose components, with a loss of about 6.3%.⁵ Stage IV (700–900 $^{\circ}\text{C}$) corresponded to the decomposition of inorganic substances such as carbonates, metal carboxylates, or certain hydrated silicate minerals, with a loss of about 4.0%.⁵ In comparison, the sludge preheated at 300 $^{\circ}\text{C}$ showed almost no significant weight loss in the 200–400 $^{\circ}\text{C}$ range (as volatile organic components had already been released during pyrolysis). Its weight loss occurred in three stages: room temperature–200 $^{\circ}\text{C}$ (about 2.93%), 400–600 $^{\circ}\text{C}$ (about 5.57%), and 700–900 $^{\circ}\text{C}$ (about 3.93%). The sludge preheated at 400 $^{\circ}\text{C}$ exhibited significant weight loss in only two stages: room temperature–200 $^{\circ}\text{C}$ (about 2.65%) and 400–600 $^{\circ}\text{C}$ (about 3.57%). For SS500 and SS600, only one weight loss stage occurred from room temperature to 200 $^{\circ}\text{C}$, with weight loss rates of 2.24% and 2.21%, respectively. These results suggested that pyrolysis reduced the content of volatile organic matter in the sludge, leading to a marked decrease in mass loss during the mid-temperature stage.⁵ The pyrolysis evolution process aligned with the pattern of “active cracking” followed by “slow cracking/char formation” and ultimately mineral decomposition, as previously reported in the literature.



3.3 Characteristic analysis of concrete

3.3.1 Setting time. Fig. 3 shows that the incorporation of sludge and its pyrolyzed sludge extended both the initial (Fig. 3a) and final (Fig. 3b) setting times of cement, with a more pronounced delay as the dosage increased. The untreated SS exerted the strongest retarding effect: at a 1% dosage, the initial and final setting times were extended to about 580 min and 864 min, respectively, and at 10% they further increased to 776 min and 1101 min. In contrast, the effect of pyrolyzed sludge was weaker, with high-temperature products (SS500, SS600) showing delays similar to the baseline. This indicated that increasing the pyrolysis temperature significantly weakened the retarding effect.¹⁸ These results suggested that the addition of urban sludge, whether untreated or pyrolyzed sludge, generally delayed the hydration and setting process of cement; no admixture accelerated setting, but rather, stronger retardation occurred as the dosage increased. By contrast, high-temperature pyrolyzed sludge, particularly SS500 and SS600, had only minimal effects on setting time, indicating that the factors responsible for hydration delays in sludge were significantly reduced during thermal treatment.

The underlying reasons for this difference were twofold. First, untreated SS contained abundant organic matter and soluble phosphate salts, which reacted with calcium ions or coated cement particle surfaces, thereby hindering hydration. Second, some heavy metal ions (such as Zn^{2+}) formed poorly soluble precipitates that inhibited the hydration of cement minerals.¹⁹ The pyrolysis process decomposed or stabilized these retarding components, reducing their reactivity. In particular, under high-temperature conditions, most organic matter decomposed, while phosphorus and metal elements were transformed into insoluble forms, allowing cement hydration to proceed more normally.²⁰ In summary, untreated sludge significantly delayed cement setting, whereas the pyrolyzed sludge derived from high-temperature pyrolyzed sludge had only a limited effect. This indicated that pyrolysis not only contributed to the resource utilization of sludge but also reduced its adverse impacts on cement properties. High-temperature products ($\geq 500^\circ C$) were especially suitable for application in building materials.

3.3.2 Compressive strength. In this work, the CK group, which used P·O 42.5 ordinary Portland cement as the reference, served as a reasonable control because the compressive strengths at 3 days and 28 days fell within the typical performance range of this grade. The data show that the incorporation of different types of sludge and their pyrolyzed sludge significantly affected the compressive strength of cement specimens, and the effect varied with curing age. At 3 days (Fig. 4a), the compressive strength of CK was approximately 35.31 MPa, consistent with the expected performance of P·O 42.5 cement. The addition of untreated SS markedly reduced the early strength: at a 1% dosage, it decreased to 25.11 MPa, and at 10% it dropped to 11.52 MPa, only about one-third of the control. In contrast, the pyrolyzed sludge generally increased the 3 days strength compared with CK, with the enhancement becoming more evident at higher dosages. At 10%, SS300 reached 37.28 MPa, SS400 43.55 MPa (23% increase), SS500 48.44 MPa (37% increase), and SS600 43.02 MPa (22% increase). Among them, SS500 exhibited the most pronounced early strength gain, which can be attributed to its moderately developed pore structure and residual carbon content that enhance water retention and provide additional nucleation sites for hydration products without causing excessive dilution at a 10% replacement level.

At 28 days (Fig. 4b), all specimens exhibited strength growth with curing age. CK reached 42.73 MPa. The untreated sludge group remained below CK, with 41.45 MPa at 1% and only 30.13 MPa at 10%, showing a persistent long-term negative effect. The pyrolyzed sludge groups, however, displayed a "rise-fall" pattern with dosage. SS300 peaked at 49.56 MPa at 5%, SS400 at 53.21 MPa at 5% (24% increase), SS500 at 55.42 MPa at 3% (30% increase), and SS600 at 58.00 MPa at 1% (35% increase), indicating that the highly mineralized and ash-rich SS600 can improve strength only at low replacement levels, whereas higher dosages mainly act as an inert filler and dilute the effective clinker content. Although strength decreased beyond the optimum dosage, it remained higher than CK. These results suggest that as the pyrolysis temperature increases, the optimal dosage of sludge-derived products tends to decrease because higher-temperature products become less

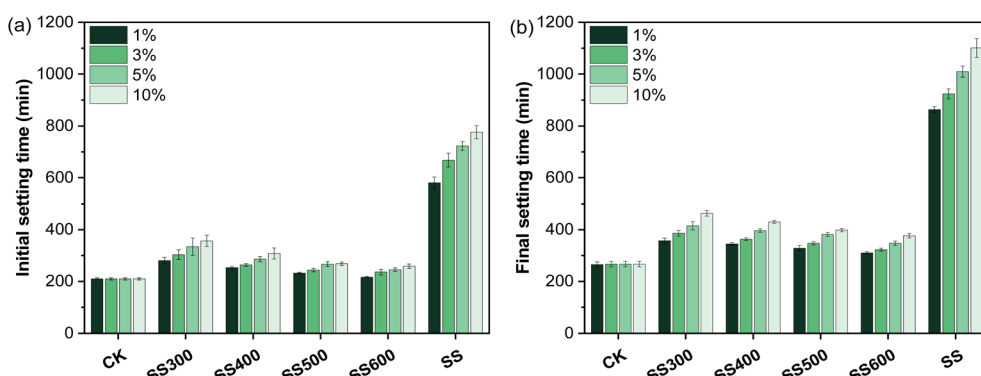


Fig. 3 Influence of replacement dosage of municipal sludge and its pyrolyzed sludge on the initial (a) and final (b) setting times of cement specimens.



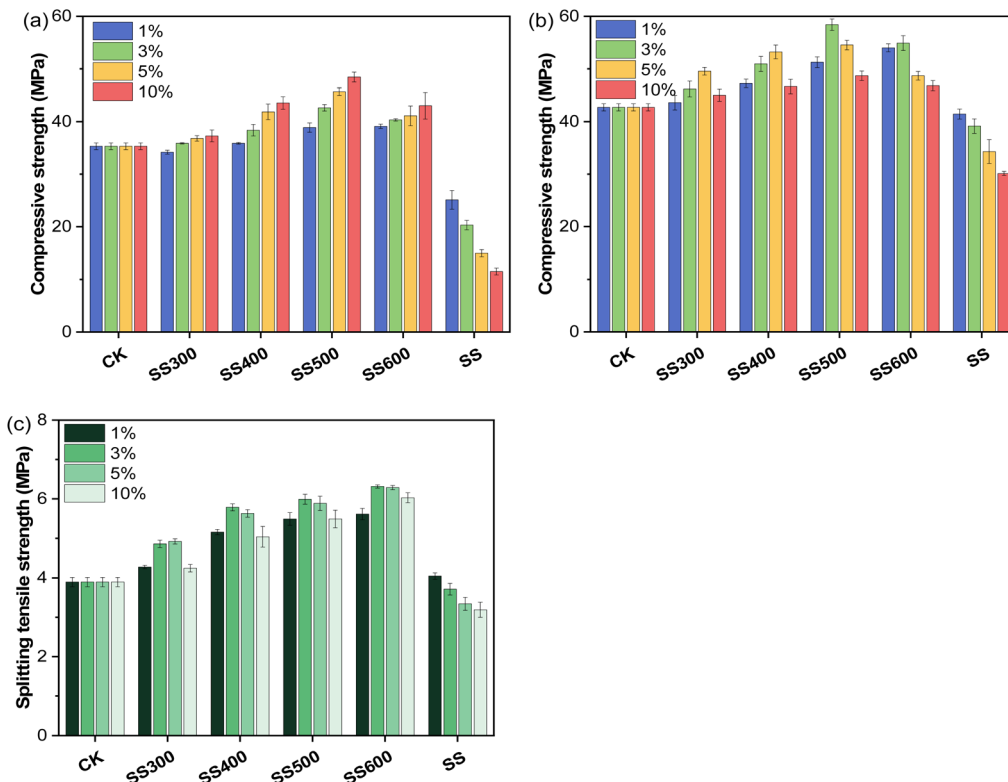


Fig. 4 Influence of replacement dosage of municipal sludge and pyrolyzed sludge on the compressive strength (a: 3 d and b: 28 d) and splitting tensile strength (c) of cement.

reactive and more ash-rich, so that excessive replacement leads to dilution of cement and strength loss.

The difference in performance arose from the distinct physicochemical characteristics of the admixtures. Untreated sludge contained abundant organic matter and soluble impurities, which interfered with cement hydration, increased porosity, and introduced interfacial defects, thereby reducing strength.²¹ By contrast, pyrolysis removed most organic matter and produced pyrolyzed sludge with porous structures and active inorganic mineral phases.²² At low to moderate dosages, these pyrolyzed sludge improved strength by filling voids, providing internal curing, and participating in pozzolanic reactions, thus densifying the cement matrix and promoting additional cementitious products. However, at higher dosages, the dilution effect and excess porosity offset these benefits, leading to a decline in strength. Untreated sludge significantly weakened both early and long-term strength, whereas pyrolyzed sludge pyrolyzed sludge, especially products obtained at 400–600 °C and applied at dosages of 1–5%, markedly enhanced the compressive strength of cement specimens.²³ Among these, SS500 and SS600 demonstrated the most notable improvements. These results indicated that pyrolysis treatment not only mitigated the adverse effects of sludge on cement properties but also promoted its resource utilization and performance optimization.

3.3.3 Splitting tensile strength. Compared with CK (Fig. 4c), the splitting tensile strength of cement blocks

prepared with dried SS and its pyrolyzed sludge at different temperatures (300, 400, 500, and 600 °C) with replacement ratios of 1% to 10% showed that: The splitting tensile strength of the CK samples remained stable at 3.89 MPa. The untreated urban sludge generally reduced the mechanical properties, and as the replacement ratio increased from 1% to 10%, the strength decreased from 4.05 MPa to 3.19 MPa, with the optimal replacement ratio being 1%. Pyrolysis treatment improved the strength, and with the increase in pyrolysis temperature, the average splitting tensile strength increased from 4.58 MPa for SS300 to 6.06 MPa for SS600. This enhancement was attributed to the increased specific surface area and porosity of the pyrolyzed sludge as the pyrolysis temperature increased, along with enhanced surface alkalinity, which facilitated the micro-filling effect and pozzolanic reactions, thereby improving the cement matrix densification. The strength of the pyrolyzed sludge increased first and then decreased with the replacement ratio. SS300 achieved the highest strength (4.92 MPa) at a 5% replacement ratio, while SS400, SS500, and SS600 reached their peak strength at 3% replacement ratios (5.79 MPa, 5.99 MPa, and 6.32 MPa, respectively). After that, as the replacement ratio increased, the strength gradually declined. This phenomenon indicated that an appropriate replacement amount could play the role of active filler, while excessive replacement diluted the cement and introduced pores, leading to a decrease in strength.^{24,25} Overall, pyrolyzed urban sludge could be used as an efficient mineral admixture, and the pyrolyzed sludge at



600 °C showed the most significant improvement in splitting tensile strength at replacement ratios of 3% to 5%. This suggested that controlling the pyrolysis temperature and replacement ratio could effectively utilize sludge resources and improve the mechanical performance of cementitious material.

3.4 Environmental risk analysis

3.4.1 Heavy metal content analysis. Urban sludge contained a certain number of heavy metals, and its incorporation inevitably influenced the background heavy metal content in cement-based materials. The total contents of Cu, Cr, Ni, Cd, Pb, Zn and As in different cement specimens were therefore determined experimentally after acid digestion of the hardened paste, and the results are presented in Fig. 5. As the pyrolysis temperature increased, the heavy metals in sludge were progressively enriched in the solid phase, and this effect became more evident at 600 °C, leading to higher total heavy metal contents in the corresponding cement specimens. For instance, the Cu content increased approximately linearly as the sludge dosage rose from 1% to 10%. The Cu content in the concretes with pyrolyzed products was higher than that of the untreated sludge, and the content further increased with higher pyrolysis temperatures: at a 10% dosage under SS600, the Cu content reached approximately 37 mg kg⁻¹, whereas under SS300 it was about 14 mg kg⁻¹, and the untreated SS exhibited an even lower value. Similarly, Zn showed the highest content in concrete, reaching about 299 mg kg⁻¹ (SS600, 10% dosage), which was significantly higher than the approximately 132 mg kg⁻¹ observed when untreated sludge was added. These results indicated that pyrolysis concentrated the heavy metals in the residual solids, thereby increasing the total heavy metal content per unit mass of the product. At the same incorporation ratio, high-temperature pyrolyzed sludge introduced more heavy metals into the concrete. Notably, the behaviors of different heavy metals varied slightly. The contents of Cd and As in

untreated sludge and low-temperature pyrolyzed sludge remained extremely low (with values close to 0). However, in high-temperature pyrolyzed sludge, the contents of these elements increased. For example, the Cd content in SS600 at a 10% dosage reached approximately 1.33 mg kg⁻¹, and the As content reached about 2.40 mg kg⁻¹, whereas no Cd or As was detected under SS300 or untreated SS conditions. This may have been due to the fact that Cd and As did not concentrate to detectable levels at lower temperatures but became evident after being enriched during pyrolysis at 600 °C.

Overall, increasing the pyrolysis temperature of sludge elevated the total heavy metal content in the resulting products, thereby raising the background heavy metal content in concrete. As the incorporation ratio increased, the cumulative heavy metal content exhibited a pronounced upward trend. However, when the leaching concentrations are viewed together with the corresponding total contents, it becomes clear that only a very small fraction of the incorporated metals was released into the leachate, suggesting that most heavy metals were strongly retained within the cement matrix.

3.4.2 Heavy metal leaching concentration study. The leaching concentrations of heavy metals in concrete under different conditions were determined using an acetic acid buffer leaching method (simulating TCLP leaching under acidic conditions) to assess their release potential. The results (Fig. 6) showed that as the sludge dosage increased, the concentrations of heavy metals in the leachate also increased. At the same time, the pyrolysis temperature exerted a complex influence on heavy metal leaching behavior.

In most cases, the heavy metal leaching concentrations in concrete containing pyrolyzed sludge were higher than those with untreated sludge, and high-temperature pyrolyzed sludge was more likely to induce elevated leaching concentrations. Taking Zn as an example, at a 10% dosage the Zn concentration in untreated sludge was approximately 0.62 mg L⁻¹, while it decreased to 0.33 mg L⁻¹ with SS300. However, the

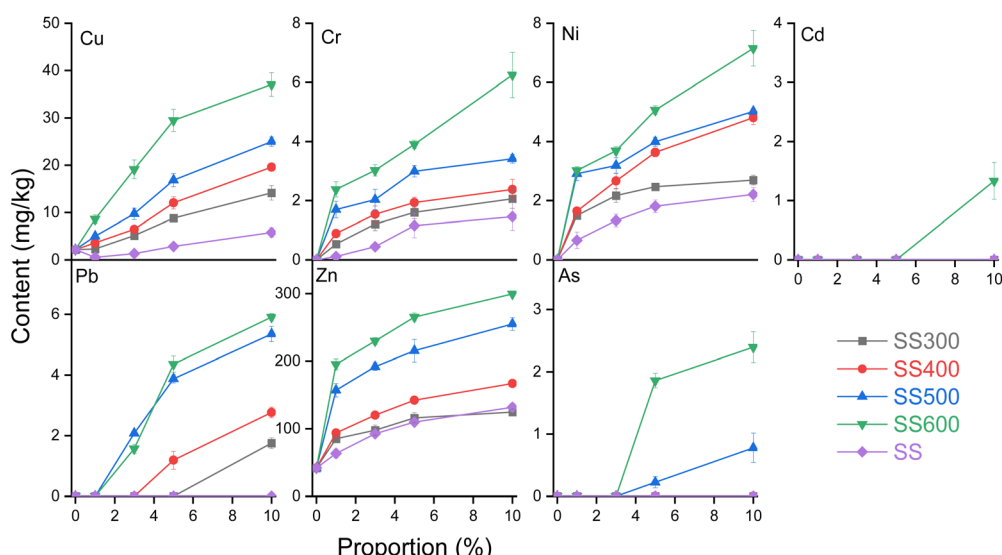


Fig. 5 Analysis of heavy metal contents in different cement specimens.



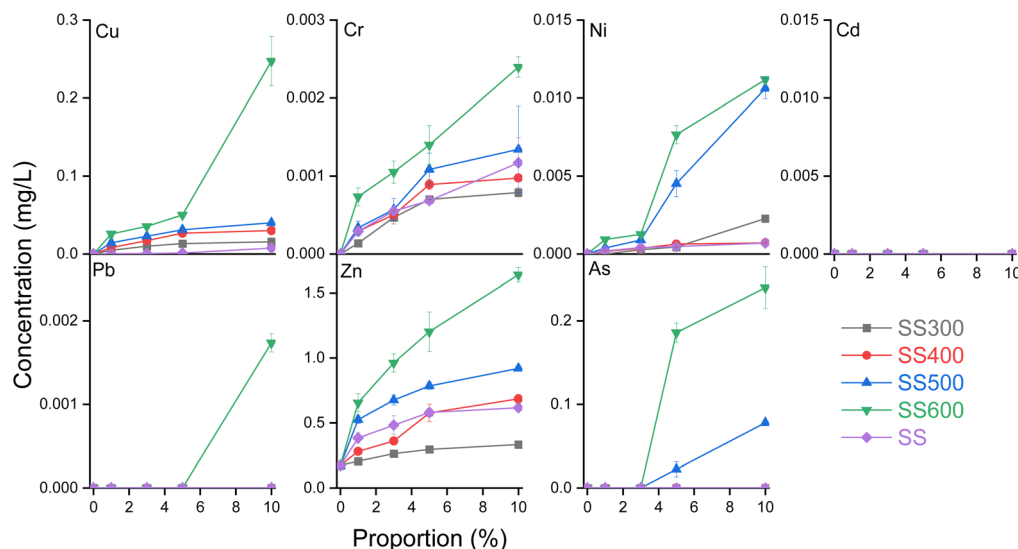


Fig. 6 Analysis of heavy metal leaching concentrations in different cement specimens.

concentrations rose to 0.69 and 0.92 mg L⁻¹ with SS400 and SS500, respectively, and peaked at 1.64 mg L⁻¹ with SS600. This suggested that low-temperature pyrolyzed sludge could, under certain conditions, slightly reduce the leaching of some heavy metals (e.g., Zn in SS300 being slightly lower than in untreated sludge), possibly due to adsorption by residual organic matter. Nevertheless, as the pyrolysis temperature increased, heavy metals in the sludge ash became more concentrated and therefore more easily leached under acidic conditions, resulting in higher leaching concentrations. Cu and Ni were particularly sensitive to pyrolysis temperature. At a 10% dosage, the Cu concentration increased from 0.007 mg L⁻¹ in untreated sludge to 0.247 mg L⁻¹ with SS600, while Ni increased from 0.0007 mg L⁻¹ to approximately 0.011 mg L⁻¹. This indicated that although high-temperature pyrolysis reduced the total organic matter, it did not stabilize metals such as Cu and Ni; instead, their enrichment during pyrolysis led to greater leaching. In contrast, the leaching concentrations of Pb and Cd remained almost undetectable (≤ 0.001 mg L⁻¹) under all conditions, implying either extremely low background levels in sludge or effective immobilization within the cement matrix. This behavior can be attributed to their relatively low baseline contents in the raw sludge and the strong stabilization of Pb and Cd in mineral phases during high-temperature pyrolysis and subsequent cement hydration. In addition, the leaching concentrations of Pb and Cd were close to the detection limits of the analytical method, so minor variations with dosage may not be fully resolved. Notably, the leaching concentration of As increased significantly under high-temperature conditions: at a 10% dosage of SS600, the As concentration reached approximately 0.24 mg L⁻¹, whereas no As leaching was detected in untreated sludge. This suggested that arsenic persisted in a form more prone to leaching after high-temperature treatment.

Overall, the heavy metal concentrations in the leachates under all conditions remained relatively low (mostly in the μ g

L⁻¹ range), indicating that the cement matrix provided a certain capacity for immobilizing and diluting heavy metals.

3.4.3 Environmental risk assessment. By jointly considering the total heavy metal contents (Fig. 5) and the leaching concentrations (Fig. 6), and comparing the latter with the limit values (Table 1) specified in the Identification Standard for Hazardous Waste: Leachability Toxicity Identification (GB 5085.3-2007), it was observed that the heavy metal concentrations under all tested conditions remained far below the standard limits. In qualitative terms, the leaching ratio, defined as the fraction of leached metal relative to its total content in the cement matrix, was very low for all elements, indicating a high immobilization efficiency.¹³ Therefore, from the perspective of leachability toxicity identification, the concretes incorporating sludge or pyrolyzed sludge did not qualify as leachability toxic hazardous waste.

Considering both the total heavy metal contents and the leaching test results, the environmental implications of sludge thermal treatment appeared two-fold. On the one hand, pyrolysis significantly reduced sludge volume and organic pollutants, while the concentrated heavy metals became encapsulated in inert carbon or ash phases and were subsequently immobilized within the cement matrix. This immobilization can be attributed to a combination of physical encapsulation of sludge-derived particles by hydration products, precipitation of metal hydroxides and carbonates under alkaline conditions, and adsorption or surface complexation on C-S-H and other cement hydrates. Within the scope of this experiment, whether or not the sludge was pyrolyzed, the heavy metal leaching concentrations after incorporation into concrete remained low and never exceeded the hazardous waste toxicity thresholds. This suggested that, with appropriate dosage control, the utilization of pyrolyzed sludge in cement-based materials was feasible, and thermal treatment did not induce excessive heavy metal leaching. On the other hand, pyrolysis increased the total heavy metal concentration in sludge, and high-temperature products even



enhanced the leaching of certain metals such as Cu, Ni, and As. This behavior is likely related to the specific speciation of these elements in high-temperature ash, which makes them weaker bound to the solid matrix and thus relatively more susceptible to acidic leaching, even though their absolute concentrations remain well below the regulatory limits. This finding highlighted the necessity of carefully considering pyrolysis temperature and its associated environmental risks in practical applications. Low-to medium-temperature products, which retained some carbon content, appeared to provide better stabilization for certain metals. By contrast, high-temperature pyrolysis maximized sludge volume reduction but required more stringent solidification measures to prevent heavy metal release.

In this work, sludge thermal treatment followed by incorporation into cement did not lead to excessive heavy metal leaching, and the environmental risk was considered controllable. A suitably selected pyrolysis process, when combined with cement solidification, effectively stabilized heavy metals and enabled the resourceful utilization of sludge.

4 Conclusion

This work showed that urban sludge could be effectively upgraded by pyrolysis and safely utilized in cement systems. Compared with previous studies that considered only a single pyrolysis condition or focused solely on mechanical properties, this work provides a systematic comparison of 300–600 °C pyrolysis products in cement paste and couples' mechanical performance with heavy metal leaching behavior to deliver an integrated mechanical–environmental evaluation. The main conclusions were as follows:

(1) Pyrolysis at 500–600 °C converted urban sludge into a more stable, porous and alkaline solid that was compatible with cement hydration and suitable for use as a partial cement replacement.

(2) Untreated sludge markedly retarded setting and reduced strength, whereas pyrolyzed sludge at 500–600 °C, used at low dosages (1–5%), mitigated the retarding effect and enhanced both early and 28 days compressive strength (maximum increases of ~37% and ~35%). Products obtained at 600 °C and dosed at 3–5% also improved splitting tensile strength, while excessive replacement remained detrimental.

(3) Although pyrolysis increased the total heavy metal contents in the solid phase, all metals were effectively immobilized in the cement matrix, and leaching concentrations of Cu, Cr, Ni, Cd, Pb, Zn and As remained far below the GB 5085.3-2007 limits.

Therefore, appropriately designed pyrolysis conditions and dosages enabled pyrolyzed sludge to serve as environmentally acceptable and performance-enhancing cement admixtures, offering a practical route for sludge reduction, stabilization and resource utilization.

Author contributions

Fangzhen Hu: investigation, conceptualization, methodology, funding acquisition, data curation, writing – original draft, writing – review & editing; Shanjun Zhang: data curation, writing – review & editing; Jing Liu: writing – review & editing.

Conflicts of interest

The authors declare no competing interests.

Data availability

Data will be made available on request.

Acknowledgements

This work was supported by Hubei Provincial Department of Science and Technology for Youths Project (2024AFB369).

References

- 1 M. Alipour, H. Asadi, C. Chen and M. R. Rashti, *Ecol. Eng.*, 2021, **162**, 106173.
- 2 Z. H. Zhang, L. Cheng, Q. X. Hu and Z. Q. Hu, *Biomass Convers. Biorefinery*, 2025, **15**, 19363–19376.
- 3 A. Zhou, S. L. Yu, S. H. Deng, H. Mikulčić, H. Z. Tan and X. B. Wang, *J. Energy Inst.*, 2023, **111**, 101417.
- 4 W. X. Zheng, M. J. Qiao, Y. F. Liu, L. Zhong, T. Chao, Q. D. Li and Y. Y. Wang, *Waste Biomass Valoriz.*, 2025, **18**, 1–10.
- 5 Q. Li, Z. P. Zhong, H. R. Du, Y. X. Yang, X. Zheng and R. Z. Qi, *J. Anal. Appl. Pyrolysis*, 2024, **181**, 106595.
- 6 T. M. Embaye, A. Zhou, R. Li, M. B. Ahmed, R. H. Ruan, D. Y. Wu, N. Deng and X. B. Wang, *Process Saf. Environ. Prot.*, 2025, **193**, 1332–1342.
- 7 Y. H. Bai, Q. H. Xia and L. F. Han, *Mater. Lett.*, 2025, **400**, 139151.
- 8 A. Yadav, P. Yadav, S. Bojjagani, J. K. Srivastava and A. Raj, *Chemosphere*, 2024, **360**, 142454.
- 9 X. Zhang, B. W. Zhao, H. Liu, Y. Zhao and L. J. Li, *Environ. Technol. Innovat.*, 2022, **26**, 102288.
- 10 A. S. Sidhu, R. Siddique and G. Singh, *Constr. Build. Mater.*, 2024, **449**, 138296.
- 11 K. Arsh, B. C. Mondal and M. M. H. Masum, *Constr. Build. Mater.*, 2025, **458**, 139454.
- 12 Y. T. Zhou, H. G. Zhang, H. T. Yang, S. Y. Li and S. He, *J. Build. Eng.*, 2025, **105**, 112375.
- 13 J. N. Shi, Z. P. Shan, Y. F. Gao, Y. R. Zhao, K. Lyu and L. Sergei, *Constr. Build. Mater.*, 2025, **490**, 142640.
- 14 Standardization Administration of China, *Test Methods for Water Requirement of Normal Consistency, Setting Time and Soundness of the Portland Cement*, GB/T 1346-2011, Beijing, 2011.
- 15 Ministry of Environmental Protection of China, *Identification Standard for Hazardous Wastes-Identification for Extraction Toxicity*, GB 5085.3-2007, Beijing, 2007.



16 X. D. Wang, Q. Q. Chi, X. J. Liu and Y. Wang, *Chemosphere*, 2019, **216**, 698–706.

17 G. H. Mo, J. Xiao and X. Gao, *Environ. Sci. Pollut. Res.*, 2023, **30**, 57771–57787.

18 Y. H. Chen, D. D. Han, G. Q. Kong, G. Chen and L. Chen, *Constr. Build. Mater.*, 2025, **489**, 140558.

19 M. İ. Tuncer, C. Başışığit and M. Davraz, *Constr. Build. Mater.*, 2025, **475**, 141102.

20 J. P. Yang, Z. P. Li, C. G. Zhao, S. N. Ouyang, B. Zuo and R. Y. Li, *Constr. Build. Mater.*, 2025, **483**, 141782.

21 M. Mottakin, S. D. Datta, M. M. Hossain, M. H. R. Sobuz, S. M. A. Rahman and M. Alharthai, *J. Build. Eng.*, 2024, **96**, 110627.

22 I. V. Fernandes, A. G. A. Gonçalves da Silva, M. D. Santos, C. F. G. Nascimento, V. M. E. Lima, R. M. Holanda and A. A. Melo Neto, *J. Build. Eng.*, 2025, **112**, 113919.

23 Y. K. Zhang, Z. Y. Ma, B. Y. Zhang, J. Q. Sun, J. D. Zhang, P. L. Ma and J. H. Yan, *Constr. Build. Mater.*, 2025, **489**, 142413.

24 X. Q. Huang, h. Yu, H. J. Wang, X. Q. Xie, C. B. Qi, F. Xue and X. R. Zhao, *Next Sustainability*, 2025, **6**, 100125.

25 X. L. Zhou, H. L. Luo, Z. P. Xu, C. W. Liu, D. Wang, Y. D. Zhang and F. Wu, *J. Clean Prod.*, 2024, **483**, 144281.

